

Original Article

Light-cured hyaluronic acid composite hydrogels using riboflavin as a photoinitiator for bone regeneration applications



Mohamed M. Abdul-Monem, PhD^{a,*}, Elbadawy A. Kamoun, PhD^b,
Dawlat M. Ahmed, PhD^a, Esmail M. El-Fakharany, PhD^c, Fayza H. Al-Abbassy, PhD^a
and Hanaa M. Aly, PhD^d

^a Dental Biomaterials Department, Faculty of Dentistry, Alexandria University, Egypt

^b Polymeric Materials Research Department, Advanced Technology and New Materials Research Institute, City of Scientific Research and Technological Applications, Egypt

^c Protein Research Department, Genetic Engineering and Biotechnology Research Institute, City of Scientific Research and Technological Applications, Egypt

^d Oral Biology Department, Faculty of Dentistry, Alexandria University, Egypt

Received 11 September 2020; revised 17 December 2020; accepted 21 December 2020; Available online 23 February 2021

المخلص

أهداف البحث: لدى العظام إمكانات محدودة للشفاء الذاتي بسبب العدوى، أو الإصابات أو الإزالة الجراحية للتكيسات. عموماً، هناك حاجة للتدخل الخارجي لزيادة إصلاح العظام وتجديدها. وتهدف هذه الدراسة لإعداد هلاميات مائية من حمض الهيالورونيك معالجة ضوئياً ومتوافقة حيويًا ومحملة بنانو هيدروكسي ابيتايت والكيوتوزان، وذلك باستخدام نظام جديد لتنشيط الفوتونات على أساس الريبوفلافين لتطبيقات تجديد العظام.

طرق البحث: تم إعداد أربع مجموعات من الهلاميات المائية معالجة بالضوء على النحو التالي: المجموعة الأولى كمجموعة ضابطة دون أي إضافات، المجموعة الثانية المحملة بالنانو هيدروكسي ابيتايت، المجموعة الثالثة المحملة بالكيوتوزان والمجموعة الرابعة المحملة بكل من نانو هيدروكسي ابيتايت وكيوتوزان. يتكون نظام تنشيط الفوتونات الجديد من الريبوفلافين كمنشط فوتوني، ميتاكاريل ديميثيلامينونيثيل كمنشط مشارك، يتم استخدامه مع الريبوفلافين للمرة الأولى وكلوريد ثنائي الفينيل أودونيوم كمنسّرع. لكل مجموعة، تم اختبار حيود الأشعة السينية، والتشكل السطحي عن طريق مسح المجهر الإلكتروني، والخصائص الميكانيكية، وامتصاص المياه (%) وقابلية الخلايا للحياة (%). ثم تم اختبار إمكانات العظام في نموذج أرنب وتم إجراء تقييم للقياسات النسيجية.

النتائج: تم الحصول في المجموعات الأربع على هلاميات مائية معالجة بالضوء بعد وقت قصير من التشيع لمدة ١٠ ثوان باستخدام وحدة علاج ضوء الأسنان. وكانت الهلاميات المائية المعدة قابلة للتكيف الحيوي. وزادت الإضافة المتزامنة لنانو هيدروكسي ابيتايت وكيوتوزان الخصائص الميكانيكية بثلاثة أضعاف، والقدرة على تكوين العظام بمقدار ضعفين مع فارق إحصائي كبير مقارنة بمجموعة التحكم.

الاستنتاجات: المركبات الهلاميات المائية المعالجة بالضوء من حمض الهيالورونيك المحملة بنانو هيدروكسي ابيتايت والكيوتوزان باستخدام نظام تنشيط الفوتونات الجديد هي مواد واعدة يمكن استخدامها في تطبيقات تجديد العظام.

الكلمات المفتاحية: تجديد العظام؛ كيوتوزان؛ هيدروجيل حمض الهيالورونيك؛ المعالجة الضوئية؛ الريبوفلافين

Abstract

Objective: Self-healing of bone from damage caused by infection, trauma, or surgical removal of cysts is limited. Generally, external intervention is needed to increase bone repair and regeneration. In this study, biocompatible light-cured hyaluronic acid hydrogels loaded with nano-hydroxyapatite and chitosan were prepared using a new photoinitiating system based on riboflavin for bone regeneration applications.

Method: Four light-cured hydrogel groups were prepared as follows: Group I, a control group with no additions; Group II, loaded with nano-hydroxyapatite; Group III, loaded with chitosan; and Group IV, loaded with both nano-hydroxyapatite and chitosan. The new

* Corresponding address: Dental Biomaterials Department, Faculty of Dentistry, Alexandria University, Alexandria, 21526, Egypt.
E-mail: mohamed.mahmoud@dent.alex.edu.eg (M.M. Abdul-Monem)

Peer review under responsibility of Taibah University.



photoinitiating system consisted of riboflavin as a photoinitiator, dimethylaminoethyl methacrylate (DMAEMA) as a coinitiator (being used with riboflavin for the first time), and diphenyliodonium chloride as an accelerator. For each group, X-ray-diffraction, surface morphology by scanning electron microscope, mechanical properties, water uptake (%), and cell viability (%) were tested. The osteogenic potential was then tested in a rabbit model, and histomorphometric assessment was conducted.

Results: In the four groups, the light-cured hydrogels were obtained after a short irradiation time of 10 s using a dental light-curing unit. The prepared hydrogels were biocompatible. Simultaneous addition of nano-hydroxyapatite and chitosan increased the mechanical properties threefold and the osteogenic potential, twofold, with a statistically significant difference compared with the control group.

Conclusions: Light-cured hyaluronic acid composite hydrogels loaded with nano-hydroxyapatite and chitosan—prepared by using the new photoinitiating system—are promising materials that can be used in bone regeneration applications.

Keywords: Bone regeneration; Chitosan; Hyaluronic acid hydrogel; Light-cured; Riboflavin

© 2021 The Authors.

Production and hosting by Elsevier Ltd on behalf of Taibah University. This is an open access article under the CC BY-NC-ND license (<http://creativecommons.org/licenses/by-nc-nd/4.0/>).

Introduction

Self-healing of bone from damage caused by infection, trauma, or cysts is limited; thus, external intervention is needed to stimulate bone repair and regeneration. Conventional methods for repairing bone defects such as autografts, allografts, and xenografts have been widely used, but they have several drawbacks that limit their clinical applications. Autografts have limited supply and present many postoperative complications, while allografts and xenografts have an increased risk of disease transmission and rejection.¹

Synthetic bone scaffolds (alloplasts) are progressively being used in bone regeneration applications to overcome the disadvantages of the previously mentioned types. Different materials can be used such as polymers (either natural or synthetic), metals, ceramics, and composites. Injectable hydrogels, which are a type of alloplasts, are hydrated networks of crosslinked polymers that offer an advantage compared with other alloplasts such as 3D solid scaffolds or membranes. Specifically, they can be used in non-invasive or minimally invasive techniques and have the ability to fill irregular bone defects.² The use of dental light-curing units for light-cured hydrogels is an attractive technique for

preparing *in situ* light-cured hydrogels for bone regeneration applications.

Hyaluronic acid has been widely used to prepare hydrogels for bone and cartilage regeneration due to its osteoconductive properties.³ It is a hydrophilic polysaccharide made of *D*-glucuronic acid and *N*-acetyl-*D*-glucosamine, and is one of the main components of the extracellular matrix of several tissues such as epithelial and connective tissues.⁴ Modification of hyaluronic acid by adding fillers is mandatory to improve its low mechanical properties and fast rate of degradation. Fillers such as bioactive nano-hydroxyapatite can be used. A nano-hydroxyapatite surface allows osteoblastic cell adhesion and growth; thus, new bone is formed by substitution from adjacent normal bone.⁵

Chitosan is a biopolymer that has been extensively used in tissue engineering applications because of its adjustable degradation rate, antibacterial effect, antifungal, mucoadhesive, analgesic, and hemostatic properties.^{6,7} Chitosan can be used in oral drug delivery, guided tissue regeneration, tissue engineering scaffolds, and enamel remineralisation.⁸ Chitosan can stimulate osteogenic progenitor cell chemotaxis and adhesion, thus enhancing bone regeneration.^{9,10} Accordingly, incorporation of nano-hydroxyapatite and chitosan to hyaluronic acid can increase mechanical stability and enhance osteogenic potential.¹¹

Synthetic photoinitiators are commonly used to prepare light-cured hydrogels for bone regeneration applications. However, there are concerns about their biocompatibility and limited solubility in water during processing. Riboflavin or vitamin B2 is naturally derived and absorbs visible light in the range of 220–450 nm; thus, it can act as an alternative to synthetic photoinitiators and can be used with conventional dental light-curing units.¹² Riboflavin is a type II photoinitiator; thus, a coinitiator is needed as a proton donor to initiate the polymerisation reaction. In the literature, a commonly used coinitiator with riboflavin is triethanol amine. However, there are concerns about the biocompatibility of triethanol amine. Dimethylaminoethyl methacrylate (DMAEMA) is a carboxylic acid ester with a tertiary amine group. It can be used as a new alternative coinitiator with riboflavin.¹³

In this study, biocompatible light-cured hyaluronic acid composite hydrogels were prepared based on a new photoinitiating system—with riboflavin as a photoinitiator, DMAEMA being used for the first time with riboflavin as a coinitiator, and diphenyliodonium chloride as an accelerator—to prepare hydrogels with a short irradiation time. The osteogenic potential of the prepared hydrogels was also tested in a rabbit model. The study tested the null hypothesis that loading nano-hydroxyapatite and chitosan onto light-cured hyaluronic acid hydrogels has no effect on mechanical properties and osteogenic potential.

Materials and Methods

Preparation of light-cured hyaluronic acid hydrogels

To prepare light-cured hyaluronic acid hydrogels, methacrylated hyaluronic acid copolymer (GMA-HA) was first

prepared by reacting hyaluronic acid (HA; $M_w = 10,000\text{--}15,000$ g/mol; Shanghai Jiaoyuan Industry, China) with glycidyl methacrylate (GMA; Sigma Aldrich, USA) in the presence of triethyl amine (Sigma Aldrich, USA) and tetrabutyl ammonium bromide (Sigma Aldrich, USA) as catalysts at $55\text{ }^\circ\text{C}$ and stirring for 2 h. After cooling to $25\text{ }^\circ\text{C}$, the mixture was precipitated in acetone (Tedia, USA). The precipitate was then collected and redissolved in distilled water. The precipitate (GMA-HA) was freeze-dried and stored at $4\text{ }^\circ\text{C}$ for preparation of hydrogel groups.¹⁴

Four light-cured hydrogel groups were then prepared (Table 1) using the prepared methacrylated hyaluronic acid (GMA-HA). The new photoinitiating system consisted of riboflavin 5'-monophosphate sodium salt hydrate (RF) as a photoinitiator, dimethylaminoethyl methacrylate (DMAEMA) as a coinitiator, and diphenyliodonium chloride (DPIC) as an accelerator (Sigma Aldrich, USA), which were added at the given percentages (Table 1). In groups II and IV, nano-hydroxyapatite (HAP; <200 nm; Sigma Aldrich, USA) was silanised before addition to the mixture, as described by Wang et al.¹⁵ In groups III and IV, chitosan (CS; de-acetylation degree: $<86\%$, $M_n 4.5 \times 10^5$; Ruji Biotech Development, China) was first dissolved in acetic acid before addition to the mixture.

Laboratory characterisation

Hydrogel discs (6 mm in diameter and 4 mm in height) were prepared for each group for laboratory characterisation. The hydrogel was injected into polytetrafluoroethylene molds and light-cured by a dental light-curing unit (2000 mW/cm^2 ; Denjoy DY 400, China; Figure 1). For each light-cured hydrogel group, the following laboratory characterisation tests were conducted.

X-ray diffraction (XRD)

The XRD patterns of the lyophilised light-cured hydrogels of the four groups were obtained with an X-ray diffractometer (Shimadzu XRD-6100, Japan) using copper K-alpha energy. The patterns were recorded in the range of $2\theta = 4^\circ\text{--}80^\circ$ at a speed of 5° min^{-1} .

Surface morphology examination by scanning electron microscope (SEM)

The surface morphology of the lyophilised hydrogel discs were examined with a scanning electron microscope (JEOL; JSM-6360LA, Japan). Hydrogel discs were immersed in distilled water for 24 h to swell before measurement. The discs were then lyophilised at $-90\text{ }^\circ\text{C}$ for 24 h under a pressure of 0.5 mbar. The lyophilised hydrogel discs were gold-coated using an ion sputter coater and then examined.

Mechanical properties

The mechanical properties of the light-cured hydrogels were tested using a rheometer (HAAKE MARS-III; Thermo-Fisher Scientific, USA). The oscillatory shear and

rotational flows were measured at $25\text{ }^\circ\text{C}$ by a two-plate model with a frequency sweep ranging from 0.1 to 10 Hz. The polymer-photoinitiating mixture for each of the four groups ($n = 5$) was light-cured *in situ* the measuring plate, forming light-cured hydrogel discs; after which, the storage modulus (G') was measured.

Measurement of water uptake (%)

The water uptake (%) of light-cured hydrogels was measured according to the equilibrium swelling theory of hydrogels. For each group, hydrogel discs ($n = 5$) were immersed in distilled water and weighed daily after placing filter paper on them to remove excess water to determine increase in weight and volume due to swelling. This step was repeated until no change in the hydrogel discs' weight was found and the discs reached the equilibrium swelling state. The discs were freeze-dried, and the water uptake (%) was determined according to the equation:¹⁶

$$\text{Water uptake (\%)} = (W_s - W_o) / W_o \times 100$$

where W_s is the weight of the swollen hydrogel disc, and W_o is the weight of the dried hydrogel disc.

Cell viability (%) by MTT assay

The effect of the swollen hydrogel extract on cell viability (%) of rabbit peripheral blood mononuclear cells (PBMCs) was determined by 3-(4,5-dimethylthiazol-2-yl)-2,5-diphenyl tetrazolium bromide (MTT) assay. PBMCs cells (1.0×10^3) were seeded into 96-well sterile flat bottom tissue culture micro-plates. PBMCs cells were cultured in RPMI-1640 media, supplied with 10% fetal bovine serum, and incubated at $37\text{ }^\circ\text{C}$ in 5% CO_2 for one day. Then, (50 μL) of swollen hydrogel extracts of each group were added to the cells and incubated for 48 h. After incubation, the hydrogel extract was removed, and the cells were washed thrice with PBS to remove debris and non-viable cells. Then, 200 μL of MTT solution were added per well and incubated for 5 h. Formazan crystals were then dissolved in 200 μL /well of dimethyl sulfoxide, and the absorbance (A) was measured at 550 nm using a microplate reader (Urit 660; Guanxi, China). Cell viability (%) was calculated using the following formula, with wells containing cells in media as control, without adding hydrogel extracts:¹⁷

$$\text{Cell viability(\%)} = \frac{A_{\text{Test}}}{A_{\text{Control}}} \times 100$$

In vivo osteogenic potential and histomorphometric assessment

The osteogenic potential of light-cured hyaluronic acid hydrogels was assessed *in vivo* on a femoral defect of a rabbit model. Twenty New Zealand white rabbits were used as test subjects, with five rabbits per group. For each group, auto-clave sterilised hydrogels (15 min, at $121\text{ }^\circ\text{C}$)¹⁸ were injected into a surgical defect (5 mm in diameter and 4 mm in depth)

in the right and left distal femur heads of each rabbit and light-cured *in situ* using dental light-curing unit for 10 s (Figure 2).

After eight weeks, the rabbits were euthanised via an overdose of diethyl ether, and the right and left femur heads of each rabbit were obtained. The femur heads were fixed in 10% buffered formalin, then dehydrated in ascending concentrations of ethyl alcohol from (70%–100%), followed by clearing in xylene and finally, embedded in polymethyl methacrylate (PMMA; Figure 3). Undecalcified sections (50 μ m thick) were obtained using a microtome precision cutter (Isomet 5000; Buehler, USA) and stained using Van Gieson's and Stevenel's blue stains (Sigma Aldrich, USA). A histomorphometric assessment to quantify the amount of newly formed bone was done using ImageJ software (National Institute of Health, USA) to calculate new bone area (%) in the region of interest (ROI) according to the following equation:¹⁹

$$\text{New bone area (\%)} = (\text{New trabeculae area} / \text{ROI area}) \times 100$$

Statistical analysis

Statistical analysis of the data was carried out using analysis of variance and Tukey's post hoc test for comparison between each two groups, at a significance level of 0.05. Analysis of data was done by IBM SPSS version 20.0.

Results

Preparation of light-cured hyaluronic acid hydrogels

In the four groups, hydrogel discs were obtained after 10 s of irradiation using a dental light-curing unit. The prepared light-cured hydrogel discs were 6 mm in diameter and 4 mm in height.

Table 1: Composition of the light-cured hyaluronic acid hydrogel scaffolds.

Hydrogel groups	GMA-HA (wt./v. %)	HAP (mg/mL)	CS(mg/mL)	Photoinitiating system	
				Component	Percentage
I	GMA-HA	12.5	–	Riboflavin	1 wt. %
II	GMA-HA/HAP	12.5	0.5	DMAEMA	0.025 v/v %
III	GMA-HA/CS	12.5	–	DPIC	0.5 wt. %
IV	GMAHA/CS/HAP	12.5	0.5		

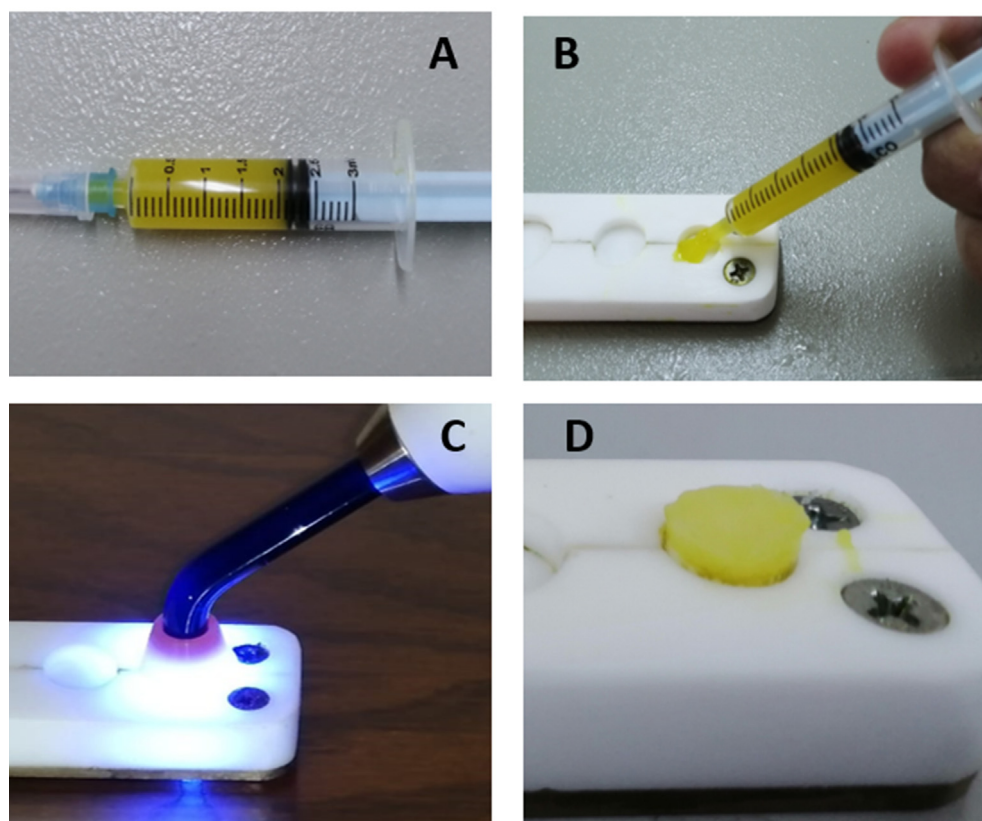


Figure 1: (A) Injectable light-cured hyaluronic acid hydrogel, (B) Injecting hydrogel into mold, (C) Light-curing using dental light-curing unit for 10 seconds, and (D) Light-cured hydrogel disc for laboratory characterisation.

X-ray diffraction (XRD)

The XRD patterns of the four hydrogel groups are presented in (Figure 4). The patterns show the amorphous nature of control group I and the semi-crystalline nature of group II as caused by the addition of crystalline nano-hydroxyapatite with characteristic peaks of nano-hydroxyapatite at $2\theta = 32^\circ$. In group III, the addition of semi-crystalline chitosan produced characteristic peaks at $2\theta = 10^\circ$ and 28° . Meanwhile, the addition of nano-hydroxyapatite and chitosan in group IV showed the same characteristic peaks as in the previously mentioned groups.

Surface morphology examination by scanning electron microscope (SEM)

The surface morphology images of the four hydrogel scaffolds are shown in (Figure 5). The SEM images revealed that

the surface morphology of group I was dense with less porosity compared with the other groups. However, the incorporation of nano-hydroxyapatite to groups II and IV led to the formation of polyhedral pores. Meanwhile, the addition of chitosan to groups III and IV resulted in the formation of a filamentous structure in the hydrogel scaffolds.

Mechanical properties

The results showed a statistically significant difference between the four groups (Figure 6, Table 2). Control group I had the lowest storage modulus at 3.48 ± 0.36 KPa. However, addition of chitosan to group III increased the storage modulus to 5.56 ± 0.53 KPa. Addition of nano-hydroxyapatite to group II resulted in a higher storage modulus (7.56 ± 0.34 KPa) than that of groups I and III. Interestingly, group IV had the highest value (10.60 ± 0.34 KPa) due to the simultaneous addition of nano-hydroxyapatite and chitosan.

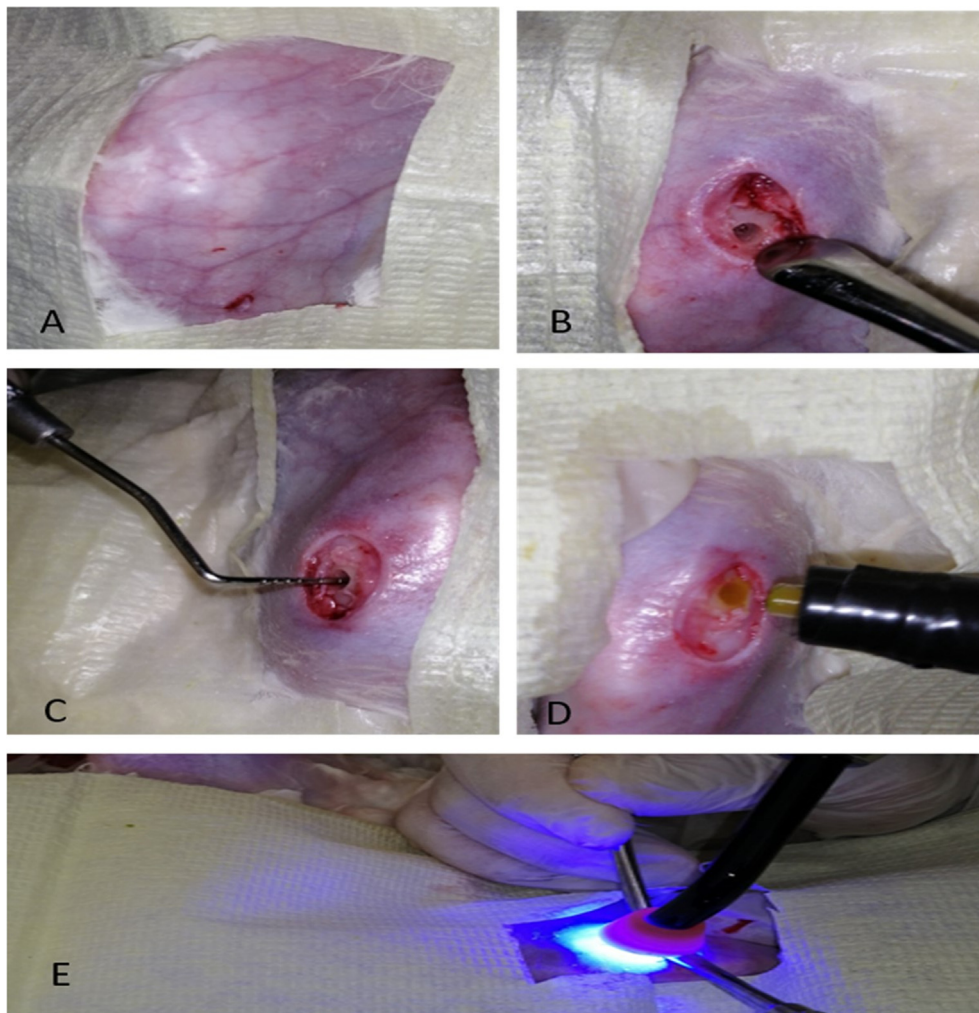


Figure 2: (A) Shaved and exposed surgical site in rabbit femur, (B) Drilled hole (5 mm in diameter and 4 mm in depth) in femur head, (C) Measuring depth and diameter of surgical defect by periodontal probe, (D) Injection of prepared hydrogel into surgical defect and (E) Light-curing hydrogel *in situ* by dental light-curing unit for 10 s.



Figure 3: Rabbit femur head embedded in PMMA for preparation of undecalcified sections.

Measurement of water uptake (%)

Water uptake (%) of the four hydrogel groups is shown in (Table 2). The equilibrium swelling state of the four hydrogel groups was reached after five days, regardless of the hydrogel composition. The water uptake (%) in the four groups was $97.04 \pm 0.11\%$, $98.46 \pm 0.18\%$, $98.38 \pm 0.26\%$, and

$98.30 \pm 0.16\%$, respectively, with no statistically significant difference.

Cell viability (%) by MTT assay

MTT assay data revealed that cell viability (%) after 48 h was the highest in group III ($83.54 \pm 0.21\%$) with a statistically significant difference compared with the other groups. In groups II and IV, cell viability (%) decreased to $73.50 \pm 0.27\%$ and $73.80 \pm 0.19\%$, respectively with no significant difference between both groups. However, cell viability (%) in control group I remained higher ($75.60 \pm 0.27\%$) than in groups II and IV, but lower than in group III, with a statistically significant difference. Cell viability (%) in all groups remained $> 70\%$ (Table 2).

In vivo osteogenic potential and histomorphometric assessment

Histological examinations of the undecalcified sections of all groups showed bone regeneration after eight weeks, at different amounts (Figure 7). The newly formed bone was seen extending from the surface of the surgical defect to the core. In the case of group I, bone formation was in the form of small islands surrounded by hydrogel remnants. In group II, undecalcified sections showed formation of thin bone trabeculae that were beginning to interconnect. In group III, undecalcified sections showed newly formed bone trabeculae at the centre of the defect. In group IV, undecalcified sections revealed that the surgical defect was filled with interconnected thick bone trabeculae formed of lamellar bone.

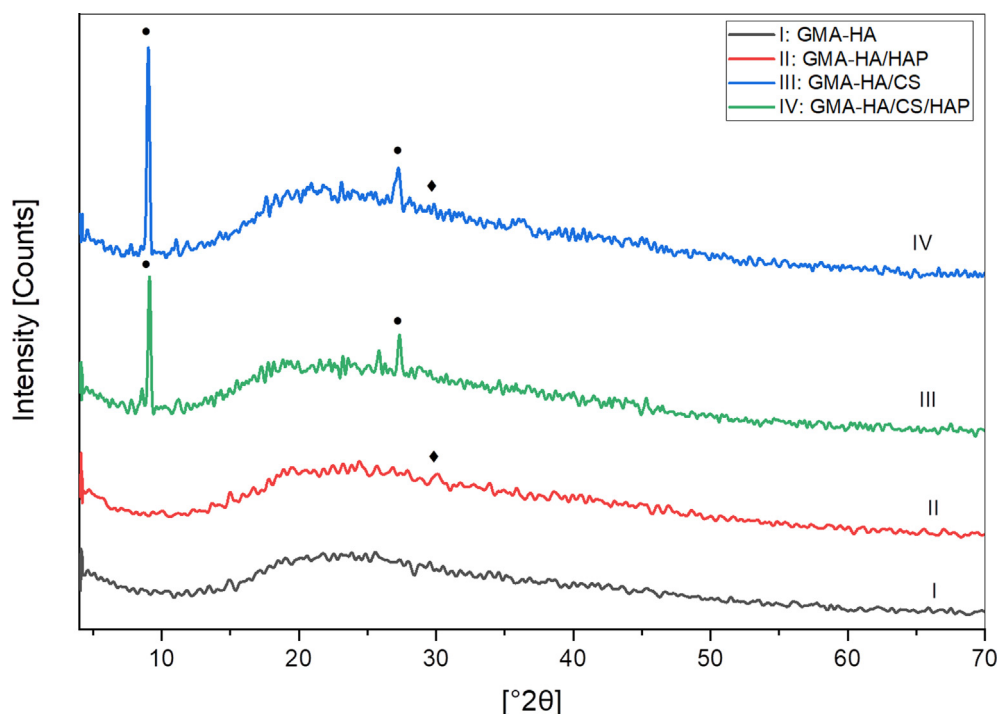


Figure 4: XRD patterns of light-cured hydrogels of the four groups, where (◆) and (●) indicate characteristic peaks of nano-hydroxyapatite and chitosan, respectively.

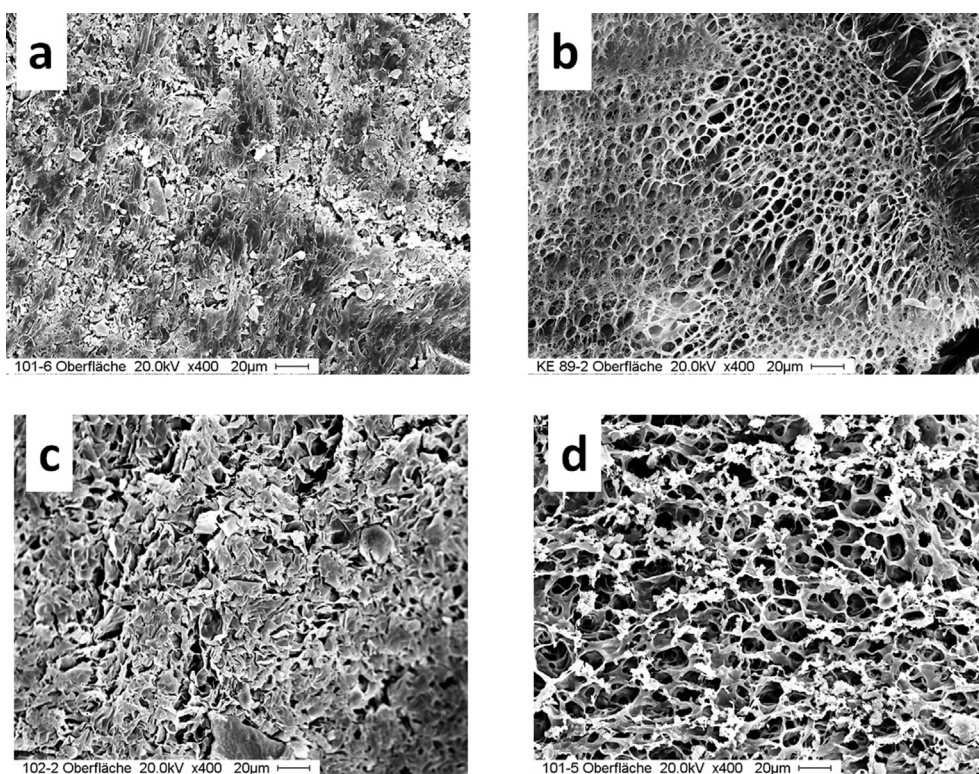


Figure 5: SEM pictures of the surface morphology of light-cured hydrogels of the four groups (a) GMA-HA, (b) GMA-HA/HAP, (c) GMA-HA/CS, and (d) GMA-HA/CS/HAP.

Statistical analysis of the histomorphometric results (Table 2) revealed a statistically significant difference between the four groups. After eight weeks, group IV showed the highest bone-forming ability ($53.90 \pm 5.68\%$),

followed by group II ($43.63 \pm 4.55\%$). Group III showed less osteogenic potential than the former two groups ($34.15 \pm 2.25\%$), while group I showed the least potential ($26.76 \pm 2.52\%$).

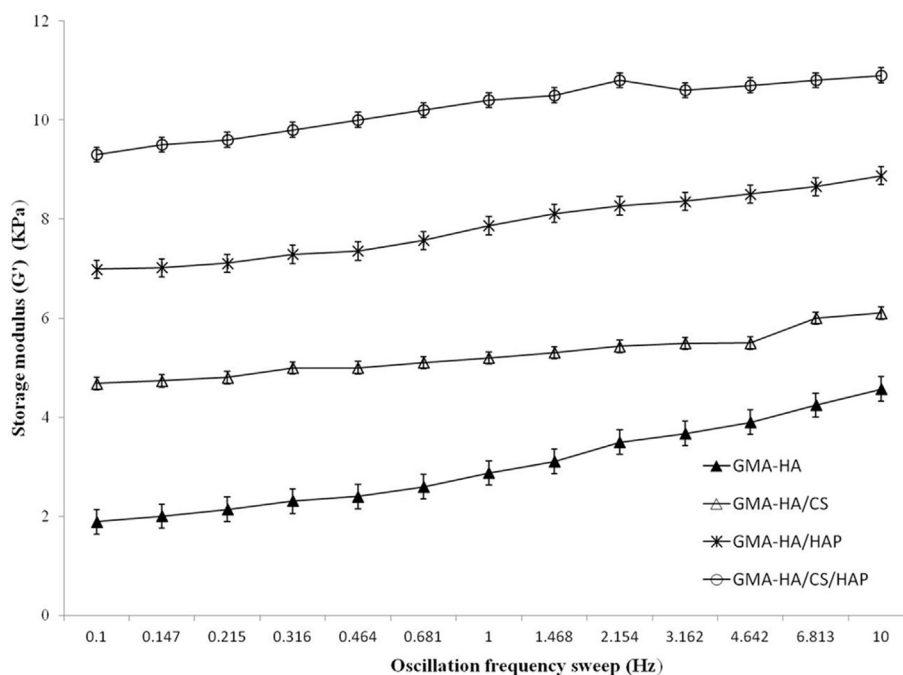


Figure 6: Storage modulus (G') of light-cured hydrogels of the four groups.

Table 2: Analysis of variance (ANOVA) using Tukey's post hoc test for pairwise comparison between each two groups (Mean \pm SD).

	Light-cured hydrogel groups			
	I: GMA-HA	II: GMA-HA/HAP	III: GMA-HA/CS	IV: GMA-HA/CS/HAP
Storage modulus (G')	(3.48 \pm 0.36) ^a	(7.56 \pm 0.34) ^b	(5.56 \pm 0.53) ^c	(10.60 \pm 0.34) ^d
Water uptake (%)	(97.04 \pm 0.11) ^a	(98.46 \pm 0.18) ^a	(98.38 \pm 0.26) ^a	(98.30 \pm 0.16) ^a
Cell viability (%)	(75.60 \pm 0.27) ^a	(73.50 \pm 0.27) ^b	(83.54 \pm 0.21) ^c	(73.80 \pm 0.19) ^b
New bone area (%)	(26.76 \pm 2.52) ^a	(43.63 \pm 4.55) ^b	(34.15 \pm 2.25) ^c	(53.90 \pm 5.68) ^d

Different letters (^{a, b, c, d}) indicate statistical difference between groups in the same row ($p < 0.05$).

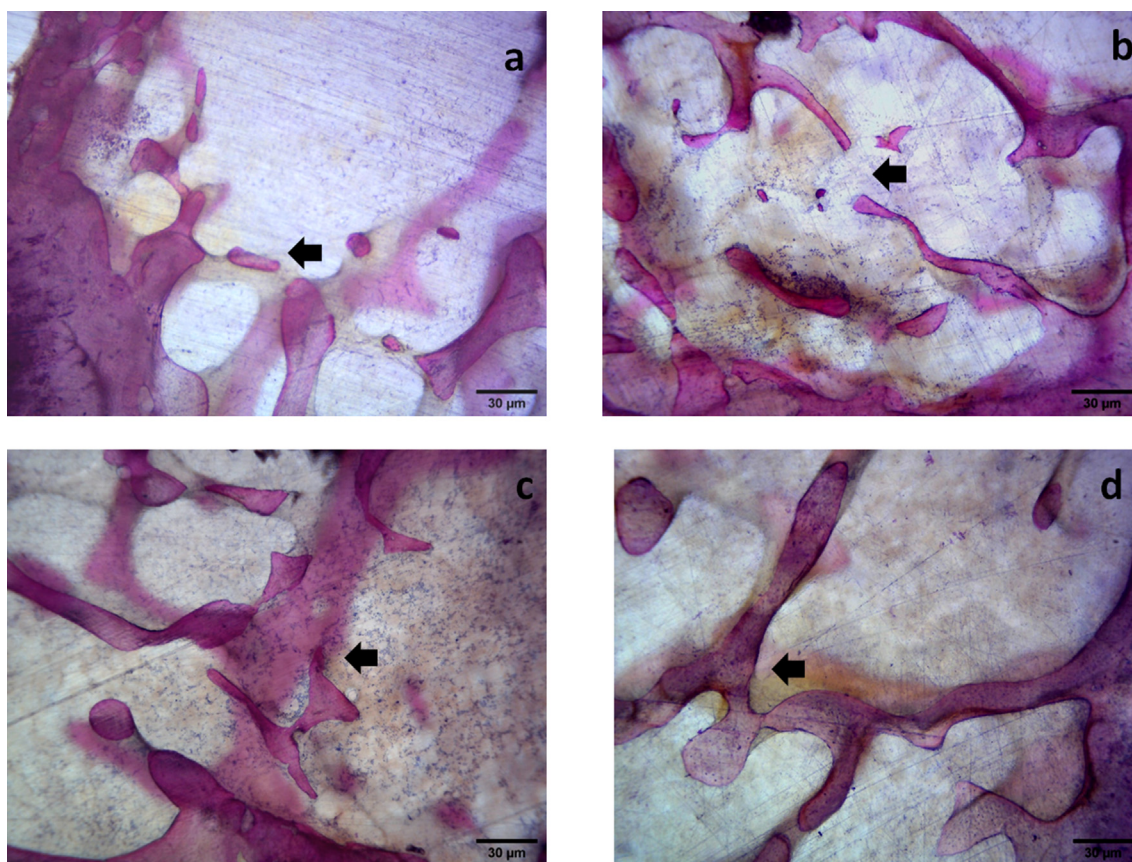


Figure 7: Photomicrographs of undecalcified sections by Van Gieson's and Stevenel's blue stains (x40); **(a)** GMA-HA, arrow showing few newly formed bone islands; **(b)** GMA-HA/HAP, arrow showing thin bone trabeculae extending from the periphery of the original bone to the centre of the defect and starting to interconnect; **(c)** GMA-HA/CS, arrow showing new bone trabeculae extending from the periphery of the original bone to the centre of the defect; **(d)** GMA-HA/CS/HAP, arrow showing thick interconnected bone trabeculae extending from the periphery of the original bone and filling the centre of the defect. Yellow-coloured parts in all sections represent the hydrogel remnants.

Discussion

Light-cured hyaluronic acid hydrogels were successfully prepared after a short irradiation time of 10 s using riboflavin as a photoinitiator, DMAEMA as a new coinitiator with riboflavin, and DPIC as an accelerator. This result of a short irradiation time is inconsistent with previous studies, such as that of Kim et al.,²⁰ who used riboflavin as a photoinitiator

with L-arginine coinitiator and obtained hydrogels after 15 min, and Chichiricco et al.,²¹ who used riboflavin with triethanol amine coinitiator and reported an irradiation time of 2 min. This short irradiation time is thought to be clinically practical for both the patient and the clinician and proves the enhanced polymerisation kinetics of the new photoinitiating system. The riboflavin photoinitiator initiates photopolymerisation in the presence of a

coinitiator such as DMAEMA, which acts as a proton donor, and DPIC improves photopolymerisation kinetics by reacting with inactive riboflavin radicals to produce active radicals, thus accelerating the polymerisation reaction.²²

Scanning electron microscope images of lyophilised hydrogel discs revealed that adding nano-hydroxyapatite led to the formation of a porous structure, which is essential for angiogenesis and cell growth. This finding is consistent with that of Huang et al.,²³ who also found that addition of nano-hydroxyapatite to glycol chitosan and hyaluronic acid hydrogels led to a porous structure. Porosity formed because the addition of nano-hydroxyapatite fillers increased the opacity of the hydrogel and decreased light penetration; thus, crosslinking density decreased and pores were formed. Meanwhile, addition of chitosan led to the formation of a filamentous structure, which is essential for osteoblast cells attachment, proliferation, and growth, as supported by the findings of Hamilton et al.²⁴

Simultaneous addition of nano-hydroxyapatite and chitosan increased the mechanical properties of light-cured hydrogels threefold, as compared with the control group. This result is in accordance with Hu et al.,²⁵ who found that simultaneous addition of nano-hydroxyapatite and chitosan to chondroitin sulfate/hyaluronic acid hydrogels increased the mechanical properties twofold, as compared with the control group. This can be attributed to the synergistic effect of the addition of silanised nano-hydroxyapatite fillers and the ionic bond formed between anionic hyaluronic acid and cationic chitosan.²⁵

Water uptake (%) in the four groups, which is approximately 98%, is thought to be sufficient, as Fricain et al.²⁶ has found that excessive swelling of hydrogels *in situ* may lead to increased pressure on tissues, opening of surgical site, and postoperative complications.

Peripheral blood mononuclear cells (PBMCs) are blood cells such as lymphocytes, monocytes, and macrophages. It is widely used in cytotoxicity assessment of materials because it is easy to obtain and is cost effective.²⁷ The MTT assay results revealed that the prepared hydrogels were biocompatible, as the cell viability (%) remained higher than 70% according to ISO 10993-5 (E).²⁸ Moreover, it was observed that cell viability (%) in group III, which was loaded with chitosan only, had the highest percentage value ($83.54 \pm 0.21\%$) after two days, with a statistically significant difference. These results corroborate those of Xu et al.,²⁹ who pointed out the positive regulatory effect of chitosan on PBMCs, *in vitro*. This result can be attributed to the featured biological activity of chitosan, namely, antibacterial, antifungal, and muco-adhesive properties.⁶ Group I showed higher cell viability (%) than groups II and IV, with a statistically significant difference. This might be attributed to the presence of free unreacted silane from silanised nano-hydroxyapatite in the latter two groups, which might have had a slight toxic effect on the cells. This finding is consistent with those of Esparza-González et al.,³⁰ who stated the dose-dependent cytotoxic effect of silane on PBMCs.

The osteogenic potential of light-cured hyaluronic acid hydrogels was tested in a rabbit femur to be able to drill

surgical defects 5 mm in diameter and 4 mm in depth without damaging any vital structures.³¹ The increased osteogenic potential of group IV hydrogel ($53.90 \pm 5.68\%$) after eight weeks is attributed to the synergistic effect of nano-hydroxyapatite and chitosan. These findings are in accordance with Zhang et al.,¹¹ who found that the use of an injectable hydrogel based on chitosan and nano-hydroxyapatite enhanced bone regeneration in rabbit femur heads after eight weeks, as compared with the use of only chitosan. The nano-hydroxyapatite surface supports osteoblastic cell adhesion and growth; thus, new bone is formed by substitution from adjacent normal bone.⁵ Meanwhile, chitosan can stimulate osteogenic progenitor cell chemotaxis, adhesion, and differentiation, thus enhancing bone regeneration.⁹

The null hypothesis was rejected, as the addition of nano-hydroxyapatite and chitosan increased the mechanical properties threefold, and the osteogenic potential, twofold, compared with the control group. In this study, histomorphometric assessment was done after eight weeks to evaluate early osteogenic potential of the prepared new hydrogels; however, further studies are needed to evaluate complete bone formation after a period of four to six months.

Conclusion

Light-cured hyaluronic acid hydrogels loaded with nano-hydroxyapatite and chitosan, using riboflavin as a photoinitiator, DMAEMA as a new coinitiator, and DPIC have high mechanical properties, high osteogenic potential, and are biocompatible; thus, they are promising materials to be used in bone regeneration applications after infections or cyst removal, as they can easily fill irregular defects.

Recommendations

Because of the high mechanical properties, biocompatibility, and osteogenic potential of the prepared light-cured hyaluronic acid hydrogels loaded with chitosan and nano-hydroxyapatite, it is recommended for use in filling irregular bone defects caused by infections or cysts. It is recommended to test the osteogenic potential of the prepared light-cured hyaluronic acid hydrogels when loaded with stem cells, growth factors such as bone morphogenetic proteins (BMPs), or bioactive materials such as nano-graphene oxide. It is also recommended to test the printability of the prepared hydrogel using the new photoinitiating system to produce 3D printed hydrogel scaffolds for bone regeneration applications.

Source of funding

This research did not receive any specific grant from funding agencies in the public, commercial, or not-for-profit sectors.

Conflict of interest

The authors have no conflict of interest to declare.

Ethical approval

The study was approved by the Ethics Research Committee of the Faculty of Dentistry, Alexandria University, Egypt (IRB No.: 00010556-IORG 0008839)/14-10-2018.

Authors' contributions

MMA and EAK conceived and designed the study, conducted research, provided research materials, collected and organised data, analysed and interpreted data, and wrote the initial and final drafts of the article. DMA and EME conducted research, collected and organised data, and analysed and interpreted data. FHA and HMA analysed and interpreted data and provided logistic support. All authors have critically reviewed and approved the final draft and are responsible for the content and similarity index of the manuscript.

References

- Bai X, Gao M, Syed S, Zhuang J, Xu X, Zhang XQ. Bioactive hydrogels for bone regeneration. *Bioact Mater* **2018**; 3: 401–417.
- Tommasi G, Perni S, Prokopovich P. An injectable hydrogel as bone graft material with added antimicrobial properties. *Tissue Eng* **2016**; 22: 862–872.
- Abid WK, Al Mukhtar YH. Repair of surgical bone defects grafted with hydroxylapatite + beta-TCP combined with hyaluronic acid and collagen membrane in rabbits: a histological study. *J Taibah Univ Med Sci* **2019**; 14(1): 14–24.
- Kogan G, Soltes L, Stern R, Gemeiner P. Hyaluronic acid: a natural biopolymer with a broad range of biomedical and industrial applications. *Biotechnol Lett* **2007**; 29: 17–25.
- Kattimani VS, Kondaka S, Lingamaneni KP. Hydroxyapatite–Past, present, and future in bone regeneration. *Bone Tissue Regen Insights* **2016**; 7: 9–19.
- Venkatesan J, Vinodhini PA, Sudha PN, Kim SK. Chitin and chitosan composites for bone tissue regeneration. *Adv Food Nutr Res* **2014**; 73: 59–81.
- Sheikh Z, Najeeb S, Khurshid Z, Verma V, Rashid H, Glogauer M. Biodegradable materials for bone repair and tissue engineering applications. *Materials (Basel)* **2015**; 8(9): 5744–5794.
- Husain S, Al-Samadani KH, Najeeb S, Zafar MS, Khurshid Z, Zohaib S, et al. Chitosan biomaterials for current and potential dental applications. *Materials (Basel)* **2017**; 10(6): 602.
- Kim IS, Park JW, Kwon IC, Baik BS, Cho BC. Role of BMP, beta-ig-h3, and chitosan in early bony consolidation in distraction osteogenesis in a dog model. *Plast Reconstr Surg* **2002**; 109: 1966–1977.
- Qasim SB, Zafar MS, Najeeb S, Khurshid Z, Shah AH, Husain S, et al. Electrospinning of chitosan-based solutions for tissue engineering and regenerative medicine. *Int J Mol Sci* **2018**; 19(2): 407.
- Zhang X, Zhu L, Lv H, Cao Y, Liu Y, Xu Y, et al. Repair of rabbit femoral condyle bone defects with injectable nano-hydroxyapatite/chitosan composites. *J Mater Sci Mater Med* **2012**; 23: 1941–1949.
- Hong BM, Park SA, Park WH. Effect of photoinitiator on chain degradation of hyaluronic acid. *Biomater Res* **2019**; 23: 21.
- Ge X, Ye Q, Song L, Laurence JS, Spencer P. Synthesis and evaluation of a novel co-initiator for dentin adhesives: polymerization kinetics and leachables study. *JOM* **2015**; 67(1989): 796–803.
- Leach JB, Bivens KA, Patrick CW, Schmidt CE. Photocrosslinked hyaluronic acid hydrogels: natural, biodegradable tissue engineering scaffolds. *Biotechnol Bioeng* **2003**; 82(5): 578–589.
- Wang S, Wen S, Shen M, Guo R, Cao X, Wang J, et al. Aminopropyltriethoxysilane-mediated surface functionalization of hydroxyapatite nanoparticles: synthesis, characterization, and in vitro toxicity assay. *Int J Nanomed* **2011**; 6: 3449–3459.
- Park H, Guo X, Temenoff JS, Tabata Y, Caplan AI, Kasper FK, et al. Effect of swelling ratio of injectable hydrogel composites on chondrogenic differentiation of encapsulated rabbit marrow mesenchymal stem cells in vitro. *Bio-macromolecules* **2009**; 10: 541–546.
- Queiroz TB, Santos GF, Ventura SC, Hiruma-Lima CA, Gaivao IOM, Maistro EL. Cytotoxic and genotoxic potential of geraniol in peripheral blood mononuclear cells and human hepatoma cell line (HepG2). *Genet Mol Res* **2017**; 16(3): gmr16039777.
- Montanari E, Di Meo C, Sennato S, Francioso A, Marinelli AL, Ranzo F, et al. Hyaluronan-cholesterol nanohydrogels: characterisation and effectiveness in carrying alginate lyase. *N Biotech* **2017**; 37: 80–89.
- Uraz A, Gultekin SE, Senguven B, Karaduman B, Sofuoglu IP, Pehlivan S, et al. Histologic and histomorphometric assessment of eggshell-derived bone graft substitutes on bone healing in rats. *J Clin Exp Dent* **2013**; 5: e23–e29.
- Kim S, Chu CC. Visible light induced dextran-methacrylate hydrogel formation using (–)-riboflavin vitamin B2 as a photoinitiator and L-arginine as a co-initiator. *Fibers Polym* **2009**; 10: 14–20.
- Chichirico PM, Riva R, Thomassin JM, Lesoeur J, Struillou X, Le Visage C, et al. In situ photochemical cross-linking of hydrogel membrane for Guided Tissue Regeneration. *Dent Mater* **2018**; 34: 1769–1782.
- Wang Y, Spencer P, Yao X, Ye Q. Effect of coinitiator and water on the photoreactivity and photopolymerization of HEMA/camphoquinone-based reactant mixtures. *J Biomed Mater Res* **2006**; 78: 721–728.
- Huang Y, Zhang X, Wu A, Xu H. An injectable nano-hydroxyapatite (n-HA)/glycol chitosan (G-CS)/hyaluronic acid (HyA) composite hydrogel for bone tissue engineering. *RSC Adv* **2016**; 6(40): 33529–33536.
- Hamilton V, Yuan Y, Rigney DA, Chesnutt BM, Puckett AD, Ong JL, et al. Bone cell attachment and growth on well-characterized chitosan films. *Polym Int* **2007**; 56(5): 641–647.
- Hu Y, Chen J, Fan T, Zhang Y, Zhao Y, Shi X, et al. Biomimetic mineralized hierarchical hybrid scaffolds based on in situ synthesis of nano-hydroxyapatite/chitosan/chondroitin sulfate/hyaluronic acid for bone tissue engineering. *Colloids Surf B Biointerfaces* **2017**; 157: 93–100.
- Fricain JC, Granja PL, Barbosa MA, De Jéso B, Barthe N, Baquey C. Cellulose phosphates as biomaterials. In vivo biocompatibility studies. *Biomater* **2002**; 23(4): 971–980.
- Vieyra H, Juarez E, Lopez UF, Morales AG, Torres M. Cytotoxicity and biocompatibility of biomaterials based in polyhydroxybutyrate reinforced with cellulose nanowhiskers determined in human peripheral leukocytes. *Biomed Mater* **2018**; 13(4):045011.
- ISO., International Organization of Standardization. *ISO 10993-5:2009(E)-Biological evaluation of medical devices-Part*

- 5: Tests for *in vitro* cytotoxicity. ISO; 2009. ISO 10993-5:2009 (E).
29. Xu W, Han B, Liang Y, Kong X, Rong M, Liu W. The effects of carboxymethyl chitosan on the regulation of the proliferation, differentiation and cytokine expression of peripheral blood mononuclear cells. **Polym J** 2012; 45(2): 226–232.
30. Esparza-Gonzalez SC, Sanchez-Valdes S, Ramirez-Barron SN, Loera-Arias MJ, Bernal J, Melendez-Ortiz HI, et al. Effects of different surface modifying agents on the cytotoxic and anti-microbial properties of ZnO nanoparticles. **Toxicol Vitro** 2016; 37: 134–141.
31. Stubinger S, Dard M. The rabbit as experimental model for research in implant Dentistry and related tissue regeneration. **J Invest Surg** 2013; 26(5): 266–282.

How to cite this article: Abdul-Monem MM, Kamoun EA, Ahmed DM, El-Fakharany EM, Al-Abbassy FH, Aly HM. Light-cured hyaluronic acid composite hydrogels using riboflavin as a photoinitiator for bone regeneration applications. *J Taibah Univ Med Sc* 2021;16(4):529–539.